# ELECTROOSMOSIS IN MEMBRANES: EFFECTS OF UNSTIRRED LAYERS AND TRANSPORT NUMBERS

## II. EXPERIMENTAL

P. H. BARRY *and* A. B. HOPE

*From the Biophysics Laboratory, School of Biological Sciences, Flinders University, Bedford Park, South Australia*

ABSTRACT In an earlier paper, it was shown that the differences in transport numbers in membranes and adjacent solutions will result in a depletion and enhancement of the local concentration profiles at the appropriate interfaces. These should, in general, cause both current-induced volume flows and transient changes in membrane potential difference (PD). The predicted concentration changes were measured near an isolated segment of plant cell wall just after a current pulse. The current-induced volume flows observed were separated into a "transport number component" and an instantaneous, electroosmotic one for both cell walls and whole cells. For walls, the electroosmotic component contributed about 53 moles·Faraday$^{-1}$ to a total coefficient of 112 moles·Faraday$^{-1}$. For whole cells, the average electroosmotic component (for both hyperpolarizing and depolarizing currents) contributed about 38 moles·Faraday$^{-1}$ to a total of about 100 moles·Faraday$^{-1}$. There was good agreement between the magnitudes and time courses of the flows and membrane PD's predicted from the theory in the previous paper, and those measured in both cell walls and whole cells.

### INTRODUCTION

As mentioned in the previous paper (Barry and Hope, 1968 *a*), (which will henceforth be referred to as part I) unless there is *perfect* stirring, the passage of current across a membrane will cause local concentration changes at each membrane-solution interface due to differences in transport numbers in each phase. This may cause both significant changes in membrane potential and also volume flows across the membrane.

The latter should in general constitute at least part of what is normally considered as electroosmosis. Provided that there is a considerable exclusion of anions in the membrane under consideration, the concentration of cations in it should remain constant during a current pulse. The true electroosmotic component should theo-

retically reach a maximum immediately after the current is turned on. In Appendix A it is shown that the time involved is of the order of 1 $\mu$sec. In practice, however, the time taken for the current to reach a maximum is much longer than this. For plant cells of *Chara australis* this latter time constant would generally be about 10 msec (Appendix A). Thus the true electroosmotic component would be expected to reach a maximum, and later to decay to zero, within a fraction of a second of the beginning and end of the current pulse, the response time of the chart recorder pen, so that any extra transient component could be considered as due to the transport number effect.

In this paper, flows observed across both a plane membrane (a segment of cell wall) and a cylindrical cell membrane (a whole plant cell) are discussed and compared with those predicted in part I.

Changes in concentration in the vicinity of a planar segment of cell wall were measured immediately after current pulses and the effect of a vigorous flushing of bulk solution at one interface was also investigated.

Membrane potential changes were also measured during current-induced flows both for cell walls and cell membranes and will be compared with those predicted theoretically in part I.

## EXPERIMENTAL EQUIPMENT AND METHODS

### *General Equipment*

The need for a simultaneous fast-response measurement of volume flows, membrane potentials, and currents necessitated the use of a very sensitive and continuous method of measurement.

The over-all experimental set up for measuring such flows in plant cells or cylindrical cell wall tubes was as shown in Fig. 1. A more detailed diagram of the transcellular holder and phototransducer is shown in Fig. 2, the optical bench being attached to a (microscope) mechanical stage and lead-based stand.

The *Chara* cell was held firmly with silicone grease in a split-Perspex (Lucite) stopper (e.g. Osterhout, 1949; Kamiya and Tazawa, 1956; Dainty and Hope, 1959). One half of the cell was in an open chamber (total volume $\sim$ 40 cm$^3$), attached to a fixed microscope stage, to make it accessible for electrode insertion and to enable viewing of the cell with a binocular microscope (Leitz Inc., New York). The other half was in a closed Pyrex chamber (total volume $\sim$ 4 cm$^3$) connected to a thick-walled capillary tube (bore about 1.36 mm). A small bead of mercury, 2–5 mm in length, supported in equilibrium by the solution column, then obstructed a light beam from a small prefocus lens-ended bulb (Eveready type 1152, Eveready Electronics, Inc., Bloomfield, N. J.) which fell on a silicon solar cell element (type N120 CG, produced by Hoffman semi-conductors [P. R. Hoffman, Carlisle, Pa.], with a response time of less than 20 $\mu$sec). The light source was fed from a four-transistor stabilized supply circuit, itself fed from a stabilized AC supply.

Thus, the fraction of the beam (width about 1.3 mm) falling on the solar cell was proportional to changes in volume in the closed chamber, i.e., the volume of solution transported transcellularly by the cell. The current output of the phototransducer was backed off by a 110-step stabilized resetting circuit at the input to a six transistor (current) amplifier with a

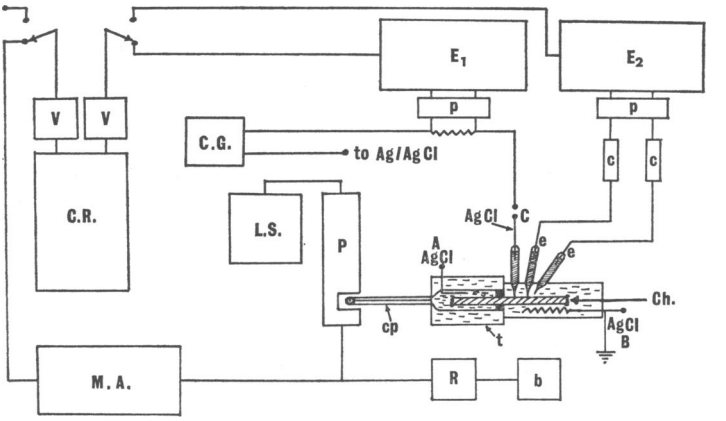


FIGURE 1 A schematic diagram of the experimental set up to measure current-induced volume flows. The notation is as follows: *Ch* refers to the *Chara* cell, *P*, photo transducer; *Cp*, capillary; *t*, thermal reservoir; AgCl, Ag/Cl electrodes; *e*, KCl-filled glass electrodes; *c*, calomel half-cells; *p*, backing-off potentiometers; $E_1$ and $E_2$ Keithley electrometers (Keithley Instruments, Inc., Cleveland, Ohio); *L.S.*, stabilized light source; *R*, resetting circuit with stabilized supply, (*b*); *M.A.*, main amplifier; *V*, voltage amplifiers, and *C.R.*, chart recorder. The current generator (*C.G.*) terminals could be connected to any combination of Ag/AgCl electrodes *A*, *B*, and *C*.

low input impedance and high negative feedback. This allowed an over-all sensitivity of about 1 ma·m$\mu$l$^{-1}$ (10 ma full scale deflection (f.s.d.)) over a range of about 1–2 $\mu$l. The calibration curves of the whole phototransducer set up were quite linear between 20–80% of the full output and all measurements were only made within that range. Since the amplification was often changed between experiments, the phototransducer was calibrated at least at the beginning of each experiment. The electro-physiological set up is also shown in Fig. 1. The current generator itself was a battery source with a high output impedance which varied from $10^6$–$10^8$ Ω depending on the current range used. This normally produced a very constant current in every experiment with the exception of some of the cell wall experiments in 0.1 and 1.0 mM KCl. This will be discussed under the third point in the section on Measurements of PD and concentration changes.

The outputs of both the main amplifier and electrometers were connected, via single stage grounded-base transistor amplifiers, to the input of a two channel Evershed and Vignoles (Evershed and Vignoles Ltd., Chiswick, London) 10 ma (3 kΩ) fast response ($\tau \leqq 0.2$ sec) chart recorder to which a secondary slow speed electric motor had been added.

Ag/AgCl electrodes, either attached to each chamber or in a 3N KCl filled glass microelectrode (5–15 $\mu$ tip), were used for passing current and 3 N KCl filled glass microelectrodes and calomel half cells were used for measuring membrane potential differences (PD's).

Because the whole transducer acts as a very sensitive thermometer (with a temperature sensitivity of about 1 m$\mu$l/0.001°C), the closed end chamber was surrounded by a thermal reservoir of solution at ambient temperature, to reduce the effect of short term temperature fluctuations. However there were still slow variations in background flow due to long term temperature fluctuations.

For planar segments of plant cell walls, the equipment was basically the same as for whole cells. However, two special double stoppers were designed for the former and the segment of cell wall was clamped firmly with silicone grease between both sections of the stoppers, leaving an effective area of about 0.038 cm$^2$ exposed. The basic design of both stoppers is shown

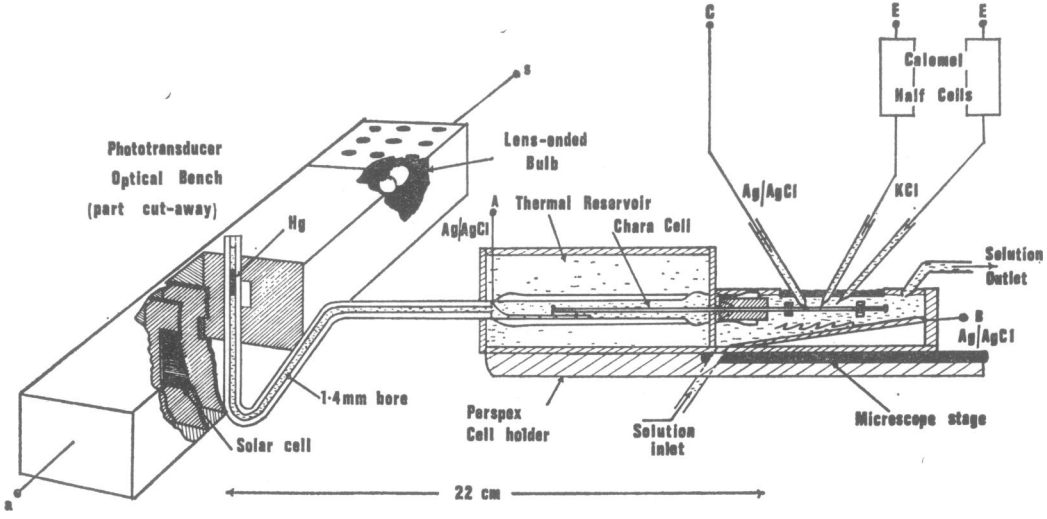


FIGURE 2 A schematic diagram of the cell holder and phototransducer used for measuring current-induced volume flows in whole *Chara* cells and cell walls (see also Fig. 1). *E* refers to the connection to the electrometers; *A*, *B*, and *C*, to the current generator; *s*, the stabilized light source supply; and *a*, the main amplifier. Further details of the set up and its operation are given in the text.

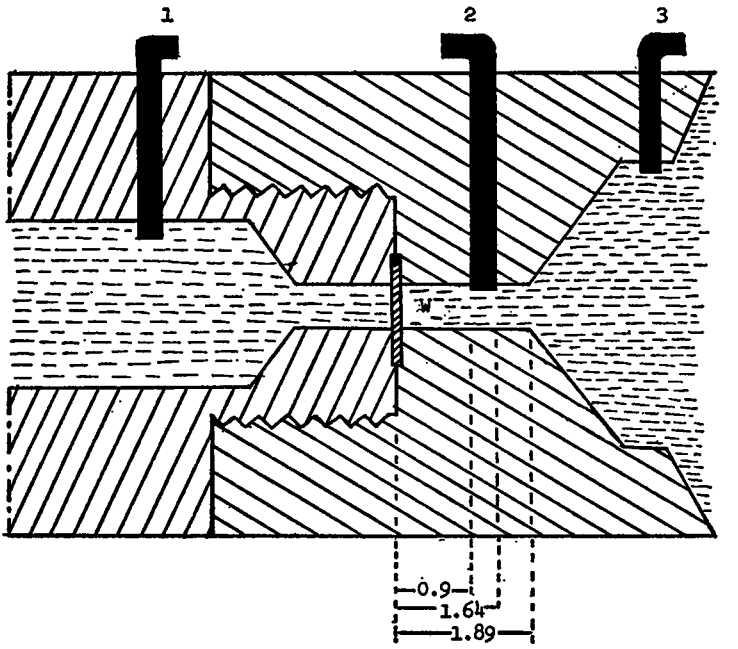


FIGURE 3 A schematic diagram of the Perspex double stoppers, used for measuring current-induced volume flow-through, and concentration changes near segments of cell walls of *Chara australis*. *W* represents the cell wall, clamped firmly, with silicone grease, between both halves of the double stopper. 1, 2 and 3 represent the three Ag/AgCl electrodes, with the dimensions and position of electrode 2 given in mm.

schematically in Fig. 3, one differing from the other in that it had an extra 1.6 cm glass tube attached to the channel at the open (right hand) end. There were three Ag/AgCl electrodes implanted with epoxy resin (a thermoplastic adhering variety) in the Perspex stoppers. Electrodes 1 and 3 were used to measure the PD across the membrane between bulk solutions and 2 and 3 for measuring concentration changes near the membrane. Current was again passed by the larger Ag/AgCl electrodes (*A* and *B* in Fig. 1) implanted in either transcellular chamber.

Normally either the cell or the cell wall was under a hydrostatic pressure difference of 3–6 mm of mercury (mercury bead and solution head). This, however, only caused a continuous volume flow if there was a leak in the stopper around the cell, and was used as a test of a good seal.

### *Theoretical Aspects of Experimental Method*

*Time Response of Equipment.* A hydrodynamic analysis was made of the time taken for the flow in the capillary to reach a maximum, taking into account the elasticity of the cell and the pressure buildup in the closed chamber necessary to overcome viscosity and inertial effects in the capillary and chamber. The upper limit for this time was about 1 msec. The analysis will be published in detail subsequently.

Since the chart recorder had a time constant of about 0.2 sec and the time constant of the

electronics was negligible (being $< 20$ $\mu$sec for the solar cell and about 75 $\mu$sec for the main amplifier) any immediate changes in flow could be measured to within a fraction of a second.

A value of the hydrodynamic Weber number (Cole, 1962) of $0.80 \times 10^{-8}$ indicates that inertial forces are negligible with respect to surface tension ones at the mercury-water and air-water interfaces and, therefore, that the shape of the boundary surface should remain constant for the typical volume flows obtained.

*Current Pathways.* Fensom and Dainty (1963) considered various pathways for current going through a cell held transcellularly and concluded that at least 90% of the current will go through both membranes at one end of the cell, along the vacuole, and out of the membranes at the other end. This was also checked experimentally and it was found in fact that at least 97% of the current takes this pathway.

*Volume Changes Due to Electrode Reactions.* As Mackay and Meares (1959) have suggested, there will be volume changes due to electrode reactions, in the solutions through which a current is being passed. Following their type of analysis, these volume flows will only cause apparent flows of less than 0.15 $\mu l \cdot coul^{-1}$ for KCl solutions and Ag/AgCl electrodes.

*Joule Heating.* Resistive heating will only cause an apparent flow of about 0.01 $\mu l \cdot coul^{-1}$ for currents of 10 $\mu a$ for this experimental set up and so may be neglected.

*Measurements of Potentials and Concentrations Near a Segment of Cell Wall.* In each case the potentials were measured with Ag/AgCl electrodes. Now the potential $E$ of an Ag/AgCl electrode in contact with a solution of chloride activity, $a_{Cl}$, is given (Glasstone, 1948) by

$$E = E^{\circ} - \frac{RT}{F} \log_e a_{Cl} \cong E^{\circ} - \frac{RT}{F} \log_e C_{Cl} \qquad (1)$$

where the approximation holds for very low concentrations (see discussion in part I). Two particular cases will be considered.

*Measurement of Transmembrane PD.* When there is a local enhancement of concentration $\Delta C_1$, on one side of a membrane and depletion $\Delta C_2$ on the other, then the potential difference, $\Delta E_b$, between two Ag/AgCl electrodes in similar bulk solutions of KCl (concentration $C$) on either side of the membrane would be given approximately by

$$\Delta E_b \cong -56 \log_{10} \frac{C + \Delta C_1}{C - \Delta C_2} \text{ in mv.} \qquad (2)$$

This may be derived by following a similar analysis to that discussed for equation 14 in part I, using the low concentration approximation, allowing for KCl diffusion PD's on either side of the membrane and making the assumption that $t_{Cl}/t_K \simeq 0.02$. This value of $t_{Cl}/t_K$ was somewhat arbitrarily chosen and is likely to be a lower limit of it. It should be noted that this equation is only used, however, to estimate the lower limit for the change in concentration across the cell wall.

*Measurement of local $Cl^-$ concentration.* If one electrode measures the bulk concentration, $C$, and the other, a concentration which has changed locally to $C + \Delta C$, then there will be a concentration gradient between them and a resulting diffusion potential. The PD of the electrode at a concentration $C + \Delta C$ with respect to that at $C$ will therefore be given by

$$\Delta E = -\frac{RT}{F}\left(1 + \frac{u_K - u_{Cl}}{u_K + u_{Cl}}\right) \log_e \frac{C + \Delta C}{C} \qquad (3)$$

where $u_K$ and $u_{Cl}$ are the mobilities of K and Cl in free solution. On substituting values for these and again using the low concentration approximation

$$\Delta E \cong -56 \log_{10} \frac{C + \Delta C}{C}. \quad (4)$$

For a Ag/AgCl electrode of finite size (e.g. electrode 2, Fig. 3) the PD measured between it and a reference electrode would be the PD between the *nearest* two points of both electrodes. A change in local concentration at an adjacent part of the former electrode would merely cause a local current to flow between it and the near point on that electrode, the resistive drop in the solution balancing the change in PD due to this hyper-local concentration gradient. Hence, it would be expected that, in the stopper shown in Fig. 3 electrode 2 would effectively measure the concentration at a distance of about 1.64 mm from the cell wall.

### *Materials and Methods*

The cells used were mature internodal cells of *Chara australis* obtained from Camden (New South Wales) with lengths 6.4–11.8 cm and diameters 1.14–1.36 mm. The cell wall preparations were also from cells of *Chara australis* and were of two types: cell wall tubes and segments of cell walls. The former were obtained from a cell whose contents had been completely rolled out with a polyethylene roller, washed clean, filled with 200 mM sucrose and 0.1 mM or 1.0 mM KCl solutions, and then tied off at both ends under a slight hydrostatic pressure gradient but zero osmotic pressure difference. These wall tubes were then placed in the low concentration pure KCl solutions and seemed to remain turgid enough for transcellular experimental work for quite a few hours. The segments of cell walls were cut from both whorl and internodal cells, washed in 0.1 or 1.0 mM KCl solutions, and then blotted thoroughly.

For cell walls the magnitude of the current pulses varied from 5.0–1,000 $\mu a \cdot cm^{-2}$ (Table I), whereas for whole plant cells it varied between 1.0–33.7 $\mu a \cdot cm^{-2}$ (Table II). In both cases, pulses most generally used for fast measurements were of about 20 sec duration, and those used for slow ones were of about 200 sec duration; the chart speeds being 0.25/per second and 0.33–0.083/per minute respectively.

The experiments generally lasted about 3–6 hr and in a few cases even extended to 3 days.

The state of the cell was determined by observing its cytoplasmic streaming, its membrane PD and also any loss of turgor which tended to cause a leak at the split stopper.

TABLE I

AVERAGE VALUES OF ELECTROOSMOTIC AND MAXIMUM-RATE COEFFICIENTS FOR *CHARA* CELL WALLS IN DIFFERENT SOLUTIONS*

| Solution of KCl | Range of currents | No. of sets of experiments | Maximum-rate coefficient | Electroosmotic (e-o) coefficient | | | Max-rate/e-o |
|---|---|---|---|---|---|---|---|
| | | | | Initial | Final | Average | |
| *mM* | $\mu a.cm^{-2}$ | | $\mu l.coul^{-1}$ | $\mu l.coul^{-1}$ | $\mu l.coul^{-1}$ | $\mu l.coul^{-1}$ | |
| 0.1 | 184–492 | 3 (3) | 23 ± 3 | 11 ± 3 | 11 ± 2 | 11 | 2.1 ± 0.2 |
| 1.0 | 66–684 | 7 (4) | 24 ± 1 | 10 ± 1 | 10 ± 1 | 10 | 2.3 ± 0.2 |
| 10.0 | 118–1000 | 2 (2) | 14 ± 1 | 5 ± 0 | 9 ± 2 | 7 | 2.0 ± 0.2 |

* The numbers in brackets show the number of different cell walls used, most of which were the same as those used for the other solutions. The errors are the S.E.M.

TABLE II

AVERAGE VALUES OF THE ELECTROOSMOTIC AND MAXIMUM-RATE COEFFICIENTS FOR *CHARA* CELLS IN VARIOUS SOLUTIONS*

| Solution | Electroosmotic flows | | Maximum rate of flow | | Maximum-rate coefficient/ electroosmotic coefficient |
|---|---|---|---|---|---|
| | No. of cells | Coefficient | No. of cells | Coefficient | |
| | | $\mu l.coul^{-1}$ | | $\mu l.coul^{-1}$ | |
| APW‡ | 2 | 7.6 ± 0.5 | 2 | 18.5 ± 4.4 | 2.5 ± 0.3 |
| 1.0 mN NaCl 0.1 mN KCl | 6 | 7.9 ± 0.9 | 6 | 16.4 ± 1.2 | 2.2 ± 0.2 |
| 0.1 mN KCl | 7 | 6.0 ± 1.1 | 15 | 16.5 ± 1.8 | 2.4 ± 0.1 |
| 1.0 mN KCl | 4 | 7.3 ± 1.1 | 2 | 20.5 ± 0.3 | 2.0 ± 0.3 |

* The errors shown are the S.E.M. for the group of cells.
‡ Artificial pond water (APW).

The external solutions used for cell walls were either 0.1, 1.0 or 10.0 mM KCl with the addition of 0.1 mM KCl + 1.0 mM NaCl and APW (artificial pond water, composition: 0.1 mM KCl, 1.0 mM NaCl, and 0.1 mM $CaCl_2$) solutions for plant cells.

The apparent volume flow rate in the absence of current, which may be seen in some of the chart recordings, is primarily due to slight temperature fluctuations in the closed end chamber of the transducer because of its high temperature sensitivity (discussed in the section on Measurement of transmembrane PD).

There was no stirring in the isolated cell wall experiments. Generally this was also true for the whole cell experiments. As expected, however, a flowing external solution in the open chamber didn't seem to alter the coefficients in the latter experiments (see section on the effect of the cell wall in part I). In measuring $L_p$, the hydraulic conductivity for both cells and cell walls, the maximum, initial, flow rate was measured within a few seconds of establishing a known osmotic gradient. This initial value of the flow was used because of the prompt decrease in flow due also to the "sweeping away" effect at both internal and external membrane-solution interfaces, discussed further in the section on Discontinuities in transport numbers.

The experimental accuracy of the current-induced flow coefficient in both cases would be within about ±10%.

## MEASUREMENTS OF CURRENT-INDUCED VOLUME FLOWS IN ISOLATED CELL WALLS

When a current was passed through a cell the concurrent rate of water flow showed two components both in the direction of positive current: an instantaneous component recorded at the beginning and end of the pulse (i.e. within 0.2 sec of the initiation or termination of the current; this time delay being due to recording artifacts, i.e. the response time of the chart recorder pen) and a second one, which increased slowly during the pulse duration and then decreased slowly after its termination. These two components are somewhat separable with experience in slow

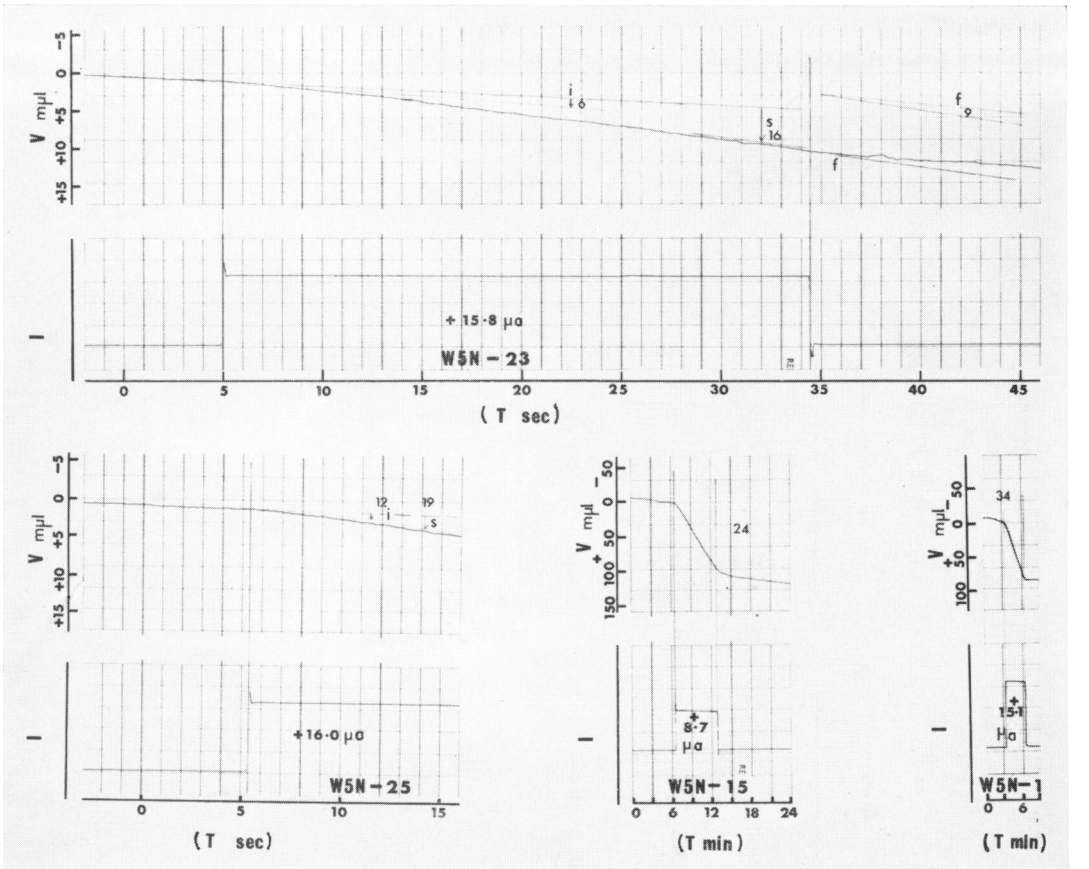


FIGURE 4 Photographs of typical fast and slow recordings of the volume, $V$ (m$\mu$l), and the currents $I$ ($\mu$a) which were passed through one segment of *Chara* cell wall, W5N, in a solution of 1.0 mM KCl. These charts show the instantaneous change in slope at the beginning and end of the fast recordings and the rather slower transient changes, which on average took about 100–160 sec to reach a maximum (see also Fig. 5). *i* and *f* refer to the initial and final changes in slope, respectively, and *s* to the maximum change in slope after 10 or 20 sec. The numbers beside them in the fast recordings refer to the appropriate current-induced coupling coefficients and in the slow recordings to the maximum coupling coefficients, each in $\mu l \cdot coul^{-1}$. Unlike the recordings shown in the later figures, these original chart traces have NOT been retouched at all for photography and reproduction.

recordings (e.g. retouched Figs. 5 *a*, run W6A-13, W6A-28 and Fig. 11, W6A-16, W6A-17, and W6A-18) but are quite distinct in fast recordings (e.g. the original untouched recordings of Fig. 4, runs W5N-23 and W5N-25), where there is a definite instantaneous initial and final change in slope. The instantaneous components in the fast recordings were of the same value as those identified from the slow recordings and are shown for a typical cell wall in Figs. 4 and 5 *b*.

In a group of experiments with isolated wall segments the values of the initial,

final and maximum rate of flow coefficients were measured and the average values for each group of experiments (each experiment being the average of about 10 current pulses in both directions) are shown in table I. The over-all number of recordings not considered to be at all useful because the background flow rate was not

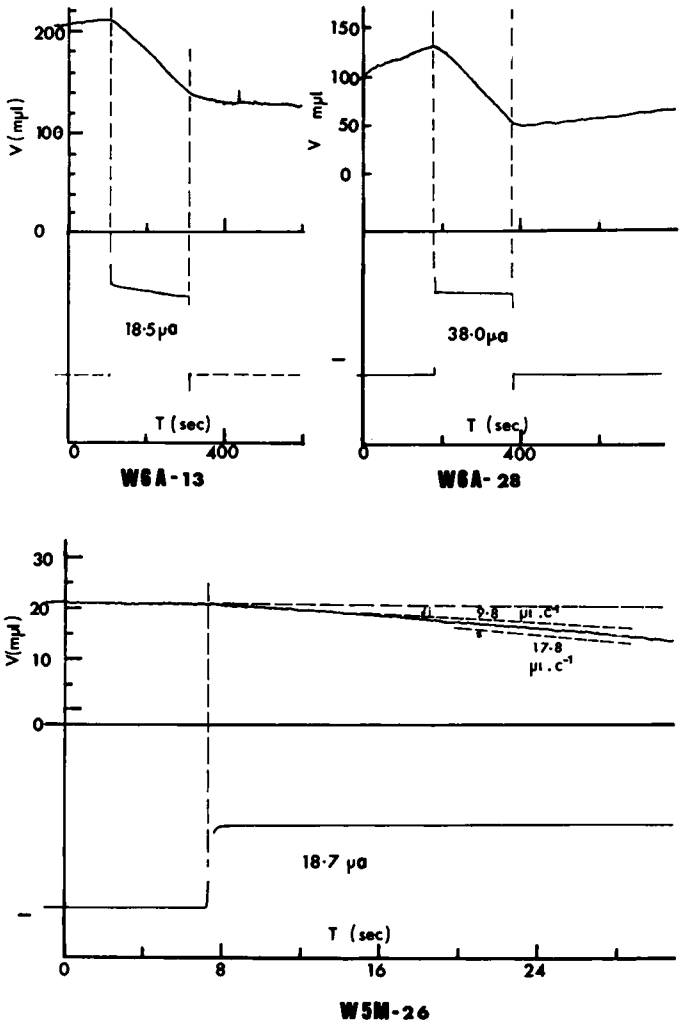


FIGURE 5 *a* Slow recordings of the volume, $V$ (m$\mu$l), and the currents, $I$ ($\mu$a), which were passed through segments of *Chara* cell walls. For run W6A-13, the wall was in 1.0 mM KCl and run W6A-28 in 10.0 mM KCl. The difference in the background slopes just before the pulse and sometime after it in these two cases was somewhat atypical and on the average was not significant (for example, cf. Fig. 4). In this and the following figures of chart recordings the fine original chart traces have been overdrawn for the purpose of photography and reproduction. 5 *b*. Typical fast recording of the volume, $V$ (m$\mu$l), and the current $I$ ($\mu$a), which was passed through segments of *Chara* cell walls in 0.1 mM KCl. The initial flow rate, $i$, and that after 30 sec, $s$, are shown with the appropriate coefficients in $\mu l \cdot coul^{-1}$.

considered stable enough (generally due to temperature problems) was between 10–20% of all those made.

The average instantaneous coefficient considered as the pure electroosmotic component was 11 ± 1 $\mu l \cdot coul^{-1}$ (or 58 moles·Faraday$^{-1}$, which for a uni-univalent electrolyte corresponds to the number of water molecules being dragged per ion) for isolated cell walls in 0.1 and 1.0 mM KCl solutions. The average maximum-rate coefficient (i.e. sum of both components) was about 23 ± 1 $\mu l \cdot coul^{-1}$ (or 122 moles·Faraday$^{-1}$). Typical time courses are shown in Figs. 4 and 5. The flows seemed to reach a maximum in times which varied from about 75 ± 11 sec for walls in 0.1 mM KCl; 70–90 sec in 1.0 mM KCl to 100–160 sec in 10.0 mM KCl.

The wall was quite symmetrical as far as the direction of current-induced flow was concerned. (cf. Gaffey and Mullins, 1958).

The coefficients at very low current densities (5–20 $\mu a \cdot cm^{-2}$) measured for cell wall tubes were comparable to those measured at much higher densities (50–600 $\mu a \cdot cm^{-2}$) for segments of cell walls. Nevertheless, for some of these higher current densities there did seem to be a slight reduction, particularly in the maximum-rate coefficient, as the current was increased. Since the current was generally increased towards the end of the experiment, there is a slight possibility that this could have been a time or hysteresis effect, or a real effect due to a change in $\alpha$ or a saturation effect ($\Delta C \rightarrow C$) at high local concentration changes and discussed in part I.

The average value of $\sigma L_p$ varied from about 3.15–4.00 $\times$ $10^{-5}$ cm·sec$^{-1}$ atm$^{-1}$ measured with a concentration gradient of 0.9 mM KCl. Making the assumption that $\sigma$(KCl) $\simeq$ 1, made plausible by estimates from KCl permeability, a comparison of these results with those for $\sigma L_p$ under sucrose gradients seemed to indicate that $\sigma$ (sucrose) varied from 0.1–0.59. These values compare reasonably well with those obtained by Tazawa and Kamiya (1965) in *Nitella flexilis* with $L_p$ varying from 1.8–3.5 $\times$ $10^{-5}$ cm·sec$^{-1}$ atm$^{-1}$ (measured under a hydrostatic gradient) and $\sigma$ (sucrose) varying from 0.20–0.52.

## MEASUREMENTS OF PD AND CONCENTRATION CHANGES IN PLANT CELL WALLS FOLLOWING A CURRENT PULSE

The same wall segments which were used for the current-induced volume flows were also used for these experiments. The change in concentration at electrode 2, after current pulses in both directions, is shown in Fig. 6 for a typical wall in a 1.0 mM KCl solution. After the termination of a positive pulse, (i.e. from electrode *A* to electrode *B*, see Fig. 2) of about 500 $\mu a \cdot cm^{-2}$ magnitude and 200 sec duration, the potential change indicated (equation 3) that the concentration at electrode 2 increased to a maximum of about 1.4 mM after 400 sec and then slowly decreased back to 1.0 mM. After a negative pulse of the same size the concentration decreased in about 40 sec to a minimum of about 0.05 mM KCl and then slowly increased again to 1.0 mM. The maximum change in concentration at the same distance from the cell wall was then plotted as a function of current pulse duration and is shown in Fig. 7 for both positive and negative currents. It reached a maximum in less than 200 sec.

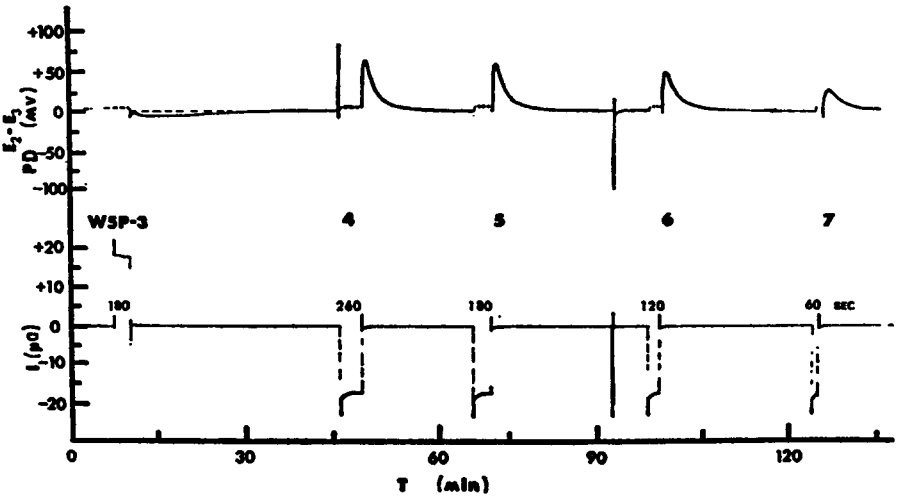


FIGURE 6 Slow recordings of the potential at Ag/AgCl electrode 2 (see Fig. 3) after current pulses of different lengths for a *Chara* cell wall segment in a 1.0 mM KCl solution. The positive potential implies a decrease in concentration and the current is defined as positive when going from electrode *A* to *B* (see Fig. 2). The dotted line on the potential trace is to signify that the electrodes were disconnected and the electrometer inputs earthed during each current pulse. It also shows the small difference between standard reference potentials of both measuring electrodes.

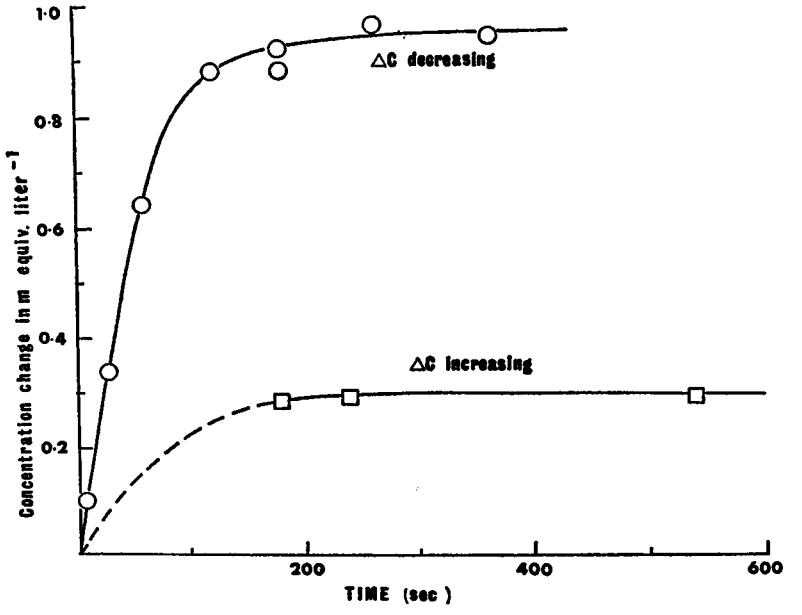


FIGURE 7 The maximum change in $Cl^-$ concentration, $\Delta C$, (mM) at electrode 2 after positive and negative current pulses through a typical wall segment in a solution of 1.0 mM. These were calculated from changes in PD similar to those shown in Fig. 6, and were plotted against the time duration of the pulses (sec).

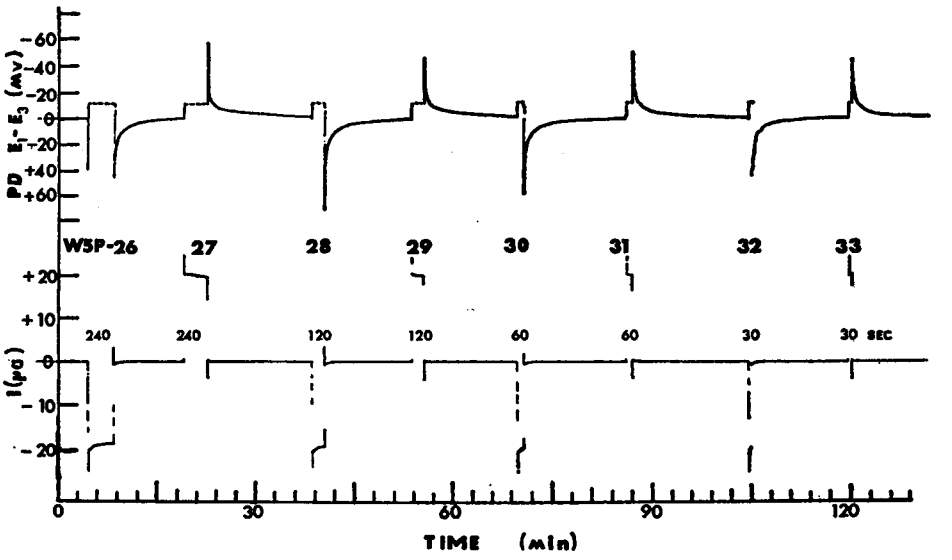


FIGURE 8 Slow recordings of the PD, $E_1$–$E_3$, across a cell wall segment in a solution of 1.0 mM KCl after pulses of various durations (indicated in sec). As in Fig. 6, the dotted line on the potential trace is to signify that the electrodes were disconnected during each current pulse.

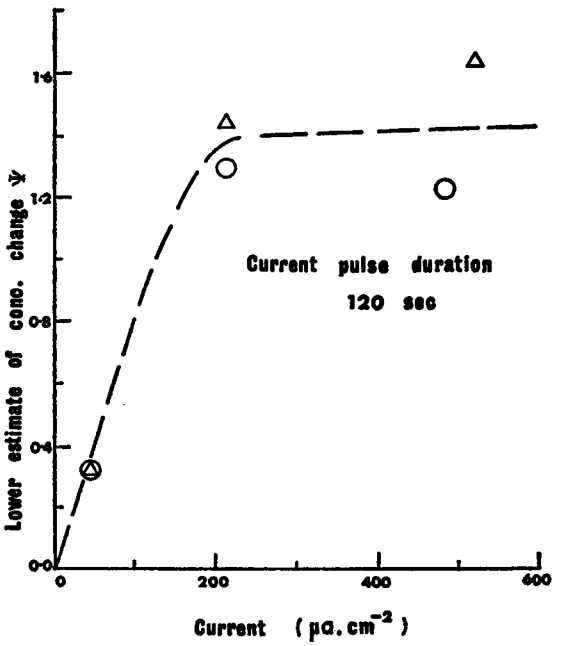


FIGURE 9 The function, Ψ a lower estimate of the change in KCl concentration (mM) across a cell wall, immediately after a current pulse. This is shown as a function of current ($\mu a \cdot cm^{-2}$) for a pulse of 120 sec in a solution of 1.0 mM KCl. The values of Ψ for negative and positive currents are shown as Δ and ○ respectively.

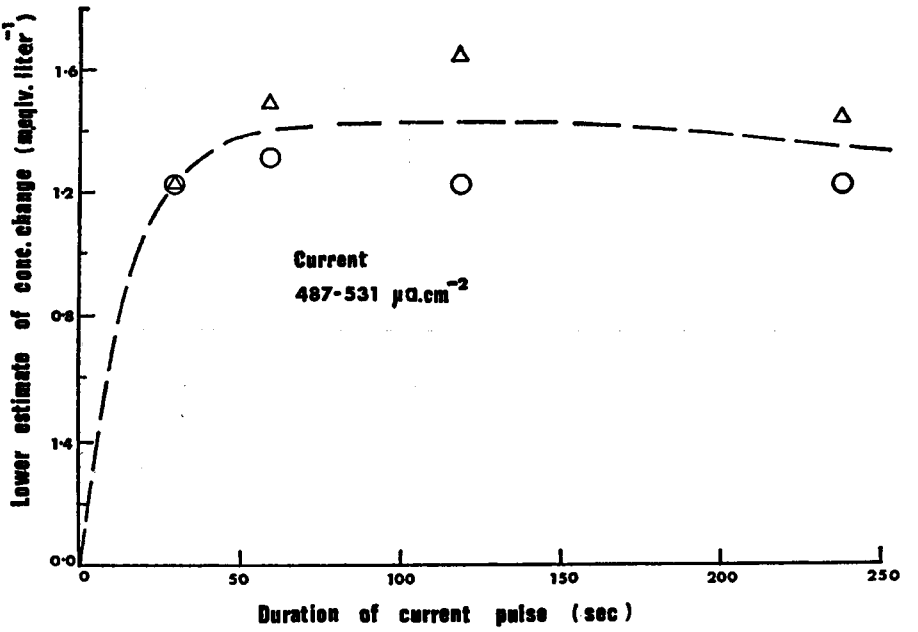


FIGURE 10 The function $\Psi$, a lower estimate of the change in KCl concentration (mM) across a cell wall, immediately after a current pulse is shown as a function of pulse duration for currents of 487–531 $\mu a \cdot cm^{-2}$. Again the values of negative and positive pulses are shown as Δ and O respectively.

The PD across the cell wall was also measured immediately after a current pulse. For positive and negative pulses, electrode 1 became positive and negative correspondingly with respect to electrode 3. At the termination of the pulse, the electrodes were connected, and the measured PD increased immediately and then slowly decreased (Fig. 8). A function, $\Psi$,[1] was defined as $2\,\Delta C$ and represents the concentration difference across the cell wall provided that the concentration changes at either interface, $\Delta C$, are equal and opposite. $\Psi$ has been plotted as a function of current magnitude and duration in Figs. 9 and 10 respectively. It seemed to reach a maximum as the current was increased from about 200–250 $\mu a \cdot cm^{-2}$ (pulse duration 120 sec) or as the pulse duration reached 40–60 sec (pulse magnitude 487–531 $\mu a \cdot cm^{-2}$).

The Perspex stopper with the long glass tube was used for one wall segment. During the current pulse, when both water flow and current were being monitored, the solution in the tube was replaced with bulk solution. This was done on one or more occasions by directing jets of solution from a syringe and polyethelene tube aimed at the cell wall and with the polyethelene tube almost touching it. As indicated in Fig. 11, such solution replacement had two effects. For a positive pulse

[1] However this function, $\Psi$, is not to be confused with the function, $\Psi$, in part I which represented the rate of solute enhancement or depletion at an interface.

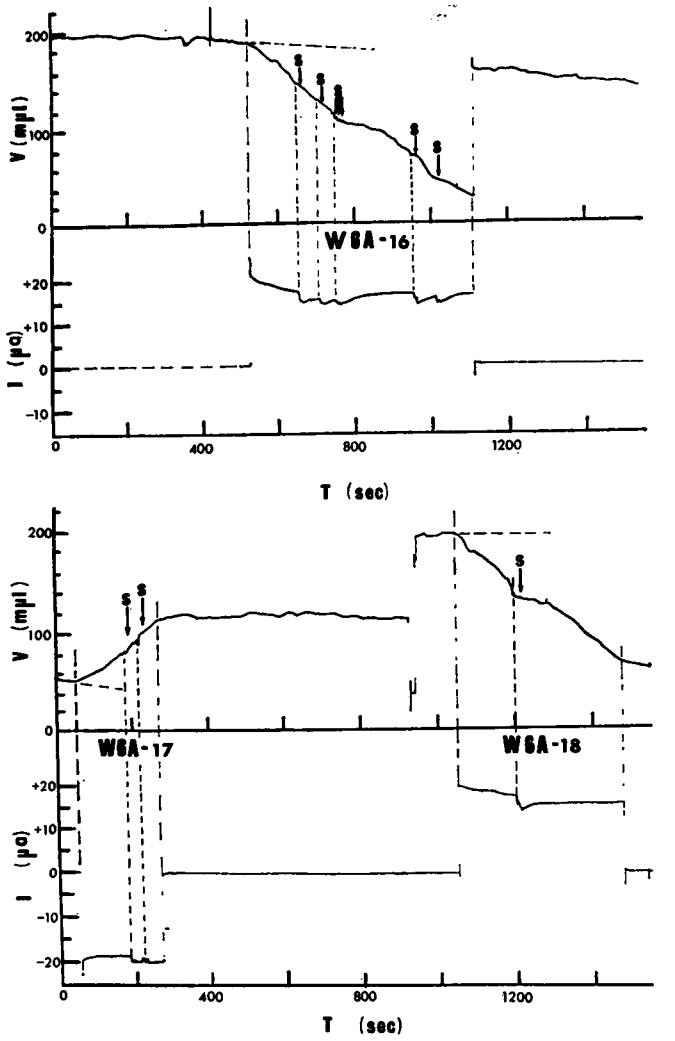


FIGURE 11 Slow recordings of the volume of water, $V$ (mμl), and the current, $I$ (μa), passed through a segment of cell wall and the effect of vigorous solution replacement (indicated by *s*) at the open end. The wall was in a solution of 1.0 mM KCl and held in the stopper with the long glass tube. For the positive pulses, W6A-16 and W6A-18 there was enhancement of the concentration at the open end. This is discussed further in the text.

(e.g. W6A-16, 18), it reduced the flow rate to about that of the electroosmotic component and decreased the current by 12–20%. For a negative pulse (e.g. W6A-17), there was very little effect on the water flow, though the current was now increased by about 8%. This may be explained as follows: In 0.1 and 1.0 mM KCl solutions, the channel resistance was of sufficient magnitude so that on the high range of the current generator (1 M Ω output resistance) significant changes in KCl concentration

in the channel close to the segments of cell wall could produce significant second order changes in the total circuit resistance seen by the first stage of the current generator. Hence, the changes in current in the experiment just described were as expected and seemed to further establish the nature of the transport number effect.

The PD across the cell wall was measured between electrodes 1 and 3 when the concentration at the closed chamber was initially 1.0 mM KCl and that in the open chamber was changed to 0.1 and 10.0 mM. The PD's were about 123 and 73 mv respectively. After subtracting the contribution due to the Ag/AgCl electrodes themselves, these values implied diffusion PD's of about 66 and 13 mv respectively. Such values implied that the concentration on the other side of the wall was about 1.5 mM instead of 1.0 mM and that $t_K/t_{Cl} \simeq 2.0$ with 10.0 mM KCl on one side.

## MEASUREMENTS OF CURRENT-INDUCED VOLUME FLOWS THROUGH WHOLE PLANT CELLS

Again the current-induced volume flows showed two components, both in the direction of positive current. The instantaneous nature of the fast component (the change in flow rate achieved within 0.2–0.4 sec of the onset or termination of the current) is shown for a typical whole plant cell in Fig. 12 and the slow nature of the second component in Figs. 13 and 14.

The average values of both of these components for transcellular currents were measured on a number of cells in four different solutions and are shown in table II. The electroosmotic coefficients were found to vary slightly around 7.2 $\mu l \cdot coul^{-1}$

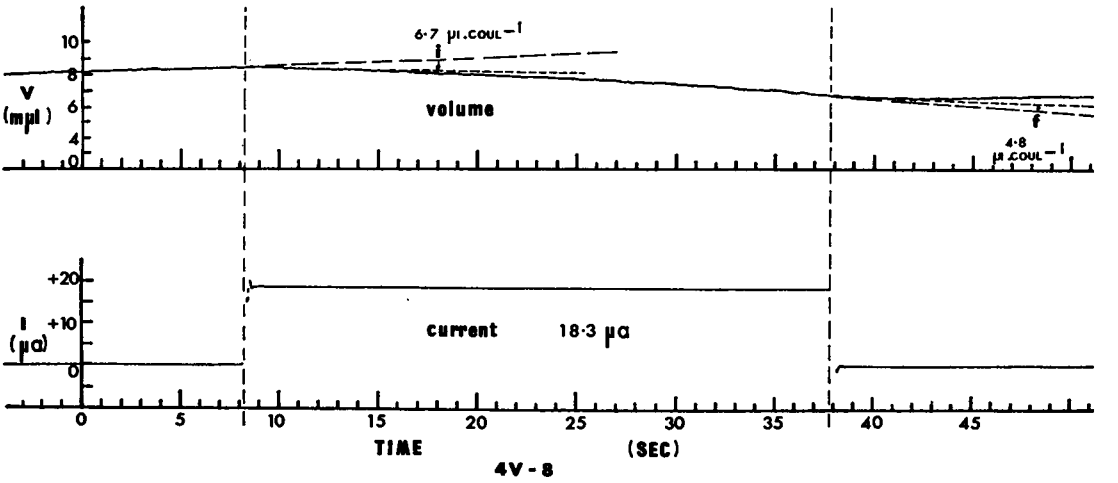


FIGURE 12 A fast recording of volume flows, $V$, (mµl), showing typical initial, $i$, and final $f$, volume flow rates through a cell of *Chara australis* in 1.0 mM KCl during a transcellular current pulse. The initial and final electroosmotic coupling coefficients are also indicated.

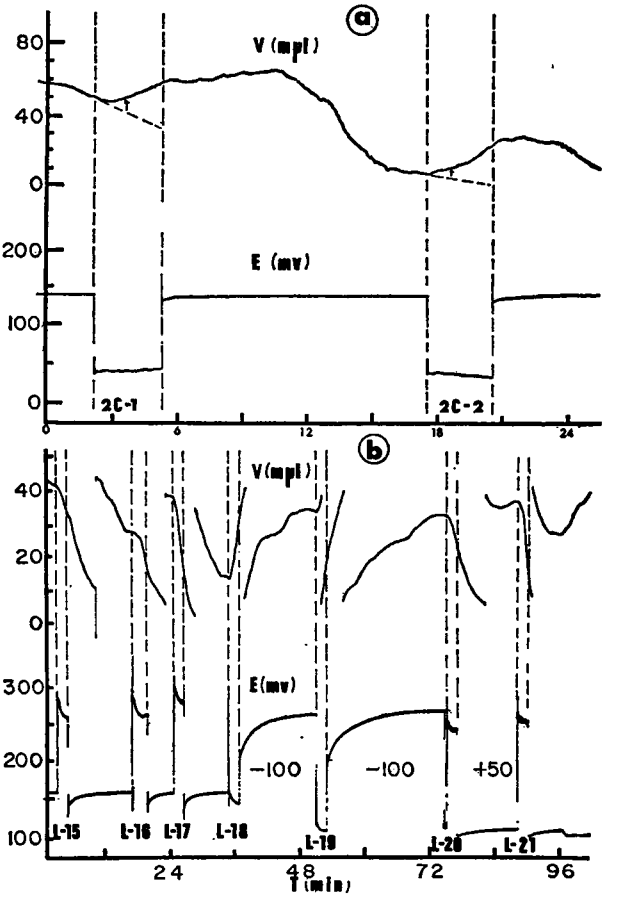


FIGURE 13 Slow recordings of volume flows, V (m$\mu$l), and membrane PD *E*, (vacuole-external solution), in mv, during transcellular current pulses through a cell of *Chara australis* in 0.1 mM KCl (Fig. 13 *a*) and in 0.1 mM KCl + 1.0 mM NaCl (Fig. 13 *b*). *a*. Positive currents of 6.4 $\mu a \cdot cm^{-2}$ were passed for 3 min, depolarizing end *B*. *b*. The cell had been previously bathed in 3 mM $MgCl_2$ for 1–1½ hr to make it inexcitable. The current pulses ranged from 3.3 to 8.2 $\mu a \cdot cm^{-2}$. For depolarizing pulses L-18 and L-19, the PD was backed-off by +100 mv, and for pulses L-20 and L-21, by −50 mv.

(38 moles · $Faraday^{-1}$)[2], whereas the value for the maximum-rate coefficient in 0.1 mM KCl solutions was about 17 $\mu l \cdot coul^{-1}$ and 20 $\mu l \cdot coul^{-1}$ in 1.0 mM KCl.

The flows again reached a maximum in about 60–150 sec during the pulse and reduced to zero in about 1.5–3 min after it. At the higher current densities there did

[2] In this paper we have considered electroosmotic coupling across the wall-membrane complex. An analysis of the actual contribution of the coupling due to the membrane itself has been undertaken by the authors and will be published subsequently. There, it will be shown that the actual coupling due to the membranes alone is 5.8 $\mu l \cdot coul^{-1}$ or 31 moles · $Faraday^{-1}$.

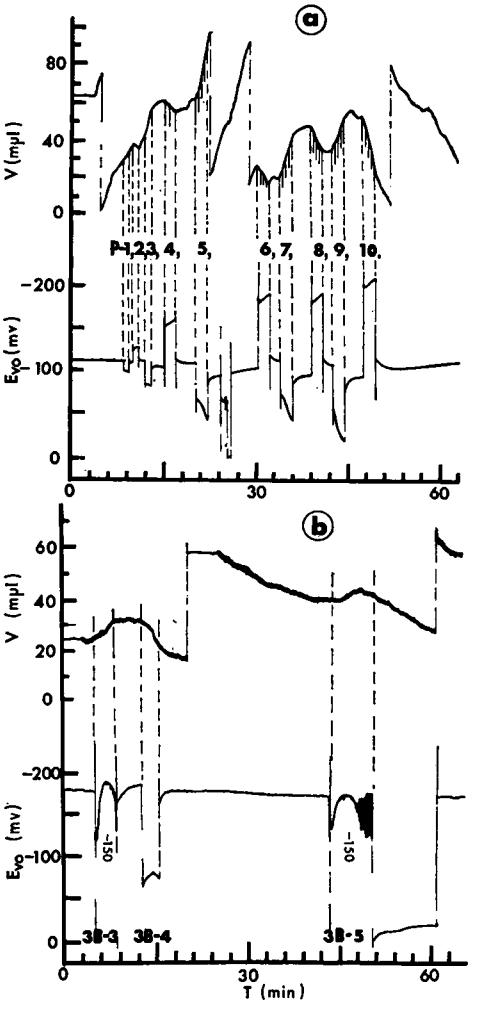


FIGURE 14 *a* A typical slow recording of volume flows, $V$ (mμl), and membrane PD, $E_{vo}$ (mv), during a number of transcellular current pulses through a cell of *Chara australis* in a solution of 0.1 mM KCl + 1.0 mM NaCl. The currents ranged from 2.7 ($P$ 1, 2) to 11.1 $\mu a \cdot cm^{-2}$ ($P$ 9, 10). Time markers are shown on the waterflow trace at the beginning and end of each current pulse; after 1 min for pulse $P$ 4 and at 30 sec intervals for pulses $P$ 5–10. 14 b A slow recording of volume flows $V$ (mμl), and membrane PD, $E_{vo}$ (mv), during transcellular current pulses through a cell of *Chara australis* in 0.1 mM KCl. The hyperpolarizing current was 3.7 $\mu a \cdot cm^{-2}$ and as indicated, the PD was backed off by 150 mv, during these pulses so that the actual PD then was $E_{vo}$-150, i.e. $\simeq$ 350 mv. The depolarizing current was 3.8 $\mu a \cdot cm^{-2}$. This shows the effect of punch-through as discussed in detail in the text. The apparent ink blot during pulse 3*B*-5 represents a train of oscillation of period, 2–3 sec.

seem to be a reduction in both coefficients, although the same remarks apply as with cell walls.

The over-all results support those of Fensom and Dainty (1963), who, though they did not recognize the two component nature of the flows, did measure maximum-rate coefficients for transcellular current in *Nitella translucens*. They also found a water flow in the direction of positive currents with coefficients varying from 5.5–47 $\mu l \cdot coul^{-1}$ (average 19 $\mu l \cdot coul^{-1}$). It was also noted that in their graph of flow rate against applied current the curves of four out of seven of their cells showed a decrease in slope with increasing current, though the others seemed quite linear up to about 40 $\mu a \cdot cm^{-2}$.

TABLE III

COEFFICIENT FOR MAXIMUM-FLOW RATE*

| Cell No. | $\Delta l/l$ | Current range | Coefficient for maximum-flow rate | | | |
|---|---|---|---|---|---|---|
| | | | Currents *A-C* and *C-B* | | | Current *A-B* |
| | | | Hyperpolarizing | Depolarizing | Total (hyperpolarizing + depolarizing | |
| | % | $\mu a.cm^{-2}$ | $\mu l.coul^{-1}$ | $\mu l.coul^{-1}$ | $\mu l.coul^{-1}$ | $\mu l.coul^{-1}$ |
| 3B | 15 | 3.2–3.5 | 4.9 ± 2.1 (2) | 7.4 ± 2.0 (3) | 12.3 ± 4.1 | 12.1 ± 2.0 (8) |
| 3E | 14 | 3.0–5.9 | 0 (2) | 3.0 ± 0.3 (2) | 3.0 ± 0.3 | 7.0 ± 2.5 (7) |
| 3F | 11 | 2.5–5.1 | 3.4 ± 1.2 (6) | 6.7 ± 1.2 (4) | 10.1 ± 2.4 | 13.2 ± 1.8 (8) |
| 3H | 10 | 5.0 | 5.5 (1) | 7.6 ± 1.2 (3) | 13.1 ± 1.2 | 5.8 ± 0.7 (2) |
| 4G | 10 | 5.3–5.4 | 6.0 ± 1.8 (3) | — | — | 16.7 ± 2.0 (5) |
| 4H | 11 | 5.5 | 8.0 ± 3.4 (4) | 15.2 ± 3.2 (3) | 23.2 ± 6.6 | 21.0 ± 2.9 (3) |
| 4K | 9 | 4.6–4.9 | 1.0 ± 1.0 (2) | 10.6 ± 3.3 (3) | 11.6 ± 4.3 | 13.1 ± 2.3 (4) |
| 4M | 9 | 4.2 | 15 ± 6 (4) | 30 ± 5 (4) | 45 ± 11 | 24 ± 5 (3) |
| Average values | | | 5.4 ± 1.9 | 11.5 ± 3.4 | 16.9 ± 5.2 | 13.7 ± 2.5 |

* The maximum-flow rate coefficients for currents going through both ends of the cell (*A-B*) and one end (*A-C* or *C-B*). $\Delta l/l$ refers to the fraction of the cell length in the stopper. The errors are again the S.E.M.

In some cells internal KCl-filled glass current electrodes were also inserted into the cells so that currents could be passed just across the membranes at one end or the other. Table III summarizes the results (the terms "hyperpolarizing" and "depolarizing" just refer to the end at which the current is being passed). The "apparent" coefficients measured for hyperpolarizing currents have an average of about 5.4 ± 1.9 $\mu l \cdot coul^{-1}$, whereas, those for depolarizing ones have an average of about 11.5 ± 3.4 $\mu l \cdot coul^{-1}$ and the sum is not significantly different from the coefficient for transcellular currents. This is to be expected as the total flow, $J_v$, should be related to the depolarizing and hyperpolarizing flows, $j_d$ and $j_h$ respectively, by

$$J_v = \frac{j_d}{2} + \frac{j_h}{2} \qquad (5)$$

where it is assumed that only a small fraction of the cell's length is in the Perspex stopper and that the cell is held symmetrically. Hence, the actual coefficients were about 11 ± 4 and 23 ± 7 $\mu l \cdot coul^{-1}$ for depolarizing and hyperpolarizing currents respectively.

The average hydraulic conductivity, $L_p$, in 11 of the cells was 0.98 ± 0.08 × $10^{-5}$ $cm \cdot sec^{-1}\ atm^{-1}$. This was similar for different osmotic gradients of both sucrose and KCl, and was consistent with the assumption that for whole cells $\sigma$ (sucrose) and $\sigma$ (KCl) $\simeq$ 1.

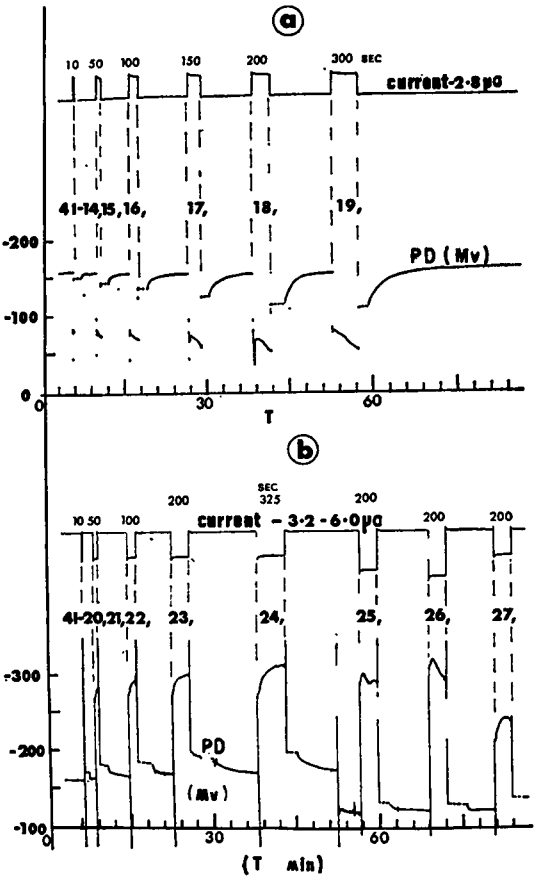


FIGURE 15 Recordings of the changes in membrane PD during and after current pulses of different duration for a cell of *Chara australis* in 0.1 mM KCl. Generally the recording was slow. Fast recordings, shown by broken traces, were used to accentuate the changes in PD Fig. 15 *a* shows the effect of depolarizing pulses and 15 *b* hyperpolarizing pulses with the punch-through phenomenon occurring for pulses 4*I*-25, 26, and 27.

## MEASUREMENTS OF CHANGES IN MEMBRANE POTENTIAL DURING THE PASSAGE OF TRANSCELLULAR CURRENT THROUGH WHOLE CELLS

During a pulse of constant current, the potential change drifted slowly as shown in Figs. 13, 14, and 15. For 10 cells in 0.1 mM KCl, the average transient change in PD for currents ranging from 1.6–5.7 $\mu$a was 30 $\pm$ 4 mv for depolarizing pulses and 23 $\pm$ 4 mv for hyperpolarizing ones, in both cases the transient change being in the direction of the initial potential change.

These transient potential changes are shown for various cells in Figs. 13, 14 *a*, and 15. There was a variation in the pattern noticed for a number of the hyperpolarizing

pulses (i.e. hyperpolarizing at the end being monitored), where the potential continued to increase slowly to about 340 mv and then suddenly reversed direction and in some instances oscillated considerably (period 2–3 sec, e.g. Fig. 14 *b*). It was noted that in some of these cases, the water flow also decreased in phase.

## A COMPARISON OF EXPERIMENTAL RESULTS WITH THEORETICAL PREDICTIONS

### *General Assessment of the Plausibility of the Theoretical Models in the Light of Known Cell Properties*

*Discontinuities in transport numbers.* Electrokinetic coupling in a membrane implies the existence of charged channels and, in general, a difference between the transport numbers of the main ions in the membrane and in the adjacent solutions. Since the mobilities of $K^+$ and $Cl^-$ are similar in bulk solution (7.9 and 7.6 $\times$ $10^{-4}$ $cm^2$ $sec.^{-1}$ $volt^{-1}$ respectively (Glasstone, 1948), and the concentrations of both ions are the same, their transport numbers will each be approximately 0.5.

In the isolated cell walls of the *Characeae*, for low concentrations of KCl, $P_K \gg P_{Cl}$ because of the ion-exchange properties of the cell walls (Dainty, Hope, and Denby 1960). This is also obvious from measurements of diffusion potentials already discussed. Hence, $t_K \simeq 1.0$ and $t_{Cl} \simeq 0$. Similarly, in the plasmalemma cell membrane of the intact cell, $P_K \gg P_{Cl}$, $P_K > P_{Na}$ (e.g. Findlay and Hope, 1964 *a*, 1964 *b*) and again $t_K \simeq 1.0$. The same may be true of the tonoplast.

The transport number changes at a wall-membrane interface and for a wall, adjacent to a membrane with a high concentration of $Ca^{++}$, have already been discussed in part I.

In intact *Characean* cells, the low values of $Cl^-$ found in the flowing cytoplasm (Kishimoto and Tazawa, 1965; Coster, 1966 *a*) may imply either fixed charges or at least relatively immobile anions, in which case there may not be a very significant discontinuity in cation transport numbers between the cytoplasm and the adjacent membranes. In any case, the relative thinness of the cytoplasm (10 $\mu$), opposite magnitudes of the concentration changes, and cytoplasmic streaming will probably not allow any significant change in concentration at either cytoplasm-membrane interface. Thus, to a first approximation, it would seem reasonable to neglect the cytoplasm and consider the cell as a cylinder with concentration changes occurring at the plasmalemma-wall interface and tonoplast-vacuole interface.

Sweeping away effects due to water flows have been observed during transcellular osmotic flows in *Nitella* by Tazawa and Nishizaki (1956) and in *Chara* by Dainty and Hope (1959), and in the present series of experiments. In fact, the effect is so marked that it will cause a backward flow almost as large as the original forward flow, after the solution with the high osmotic pressure has been replaced by the original solution. This effect is shown in Fig. 16 for one cell under a transcellular osmotic gradient

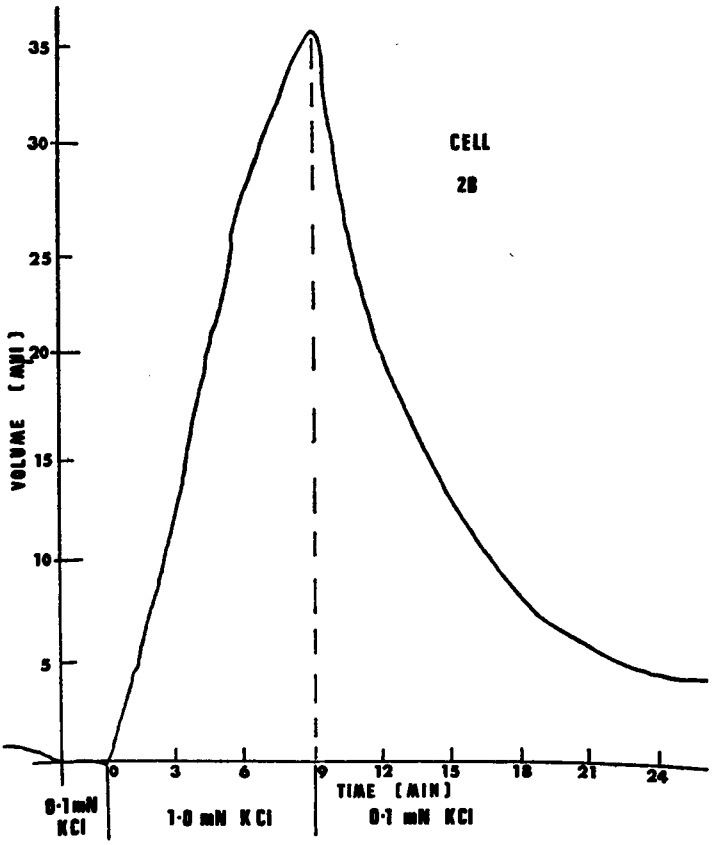


FIGURE 16 Forward and backward osmotic volume flows, V (mμl), under a transcellular concentration difference of 0.9 mM KCl. This figure was constructed from nine adjacent chart recorder scans placed together. The initial rate of flow implied that $Lp \simeq 0.85 \times 10^{-5}$ cm· $sec^{-1}$ $atm^{-1}$. The changes in solution at open end, *B*, are indicated on the time scale.

of only 0.9 mM KCl after 9 min. For flows resulting from much higher gradients, such as 0.2 M sucrose, the forward flow had almost ceased after 3–5 min. In fact, Tazawa and Nishizaki (1956) correlated their reduction in flow rate with changes in membrane potential, which they considered as being due to transcellular sap polarization of KCl.

For the isolated cell wall experiments, if a value of $5 \times 10^{-5}$ cm· $sec^{-1}$ is used for the permeability of $Cl^-$ across cell walls (Mailman and Mullins, 1966) and a value of $5 \times 10^{-4}$ cm· $sec^{-1}$ for $K^+$ (Gaffey and Mullins, 1958), then the effective permeability for KCl may be obtained from the following approximate formula

$$P_{KCl} \cong \frac{2P_K \cdot P_{Cl}}{P_K + P_{Cl}}$$

by analogy with the equation describing the electrolyte diffusion constant (Briggs et al., 1961). Hence, $P_{KCl} \simeq 9 \times 10^{-5}$ cm· $sec^{-1}$, and so the feedback factor $\beta$ ($\simeq 4\omega RT/D$) is about 10 $cm^{-1}$.

Similarly for intact plant cell membranes, where the main contribution to the feedback is due to the sweeping away effect, $\beta$ was taken as 4.0 $cm^{-1}$ corresponding to an equivalent $C_i$ of about 142 mM monovalent salt in the internal solution.

*Correlation of Experimental Results with Theoretical Predictions*

*I. Cell Walls. Volume flows.* For a feedback factor, $\beta$, of 10 $cm^{-1}$, the theoretical analysis in part I predicts values for the maximum-rate coupling coefficient of about 37 $\mu l \cdot coul^{-1}$ after about 70 sec. For small external concentrations, this will be limited by the absolute solute concentration to about 27 and 30 $\mu l \cdot coul^{-1}$ in solutions of 0.1 and 1.0 mM KCl respectively. Experimentally, for both solutions the maximum-rate coupling coefficient was about 23 $\mu l \cdot coul^{-1}$ reached in about 70–90 sec. The slight discrepancy between the experimental and predicted values may be mainly influenced by the following factors: (*a*) There could have been a decrease in $\alpha$ and increase in $\beta$ due to the production of a large PD across the wall and the increase in concentration at the enhancement side. This would have been likely since diffusion PD's did indicate a decrease in $t_K/t_{Cl}$ when the concentration on one side of the wall was increased to 10 mM. After 100 sec a typical current of about 500 $\mu a \cdot cm^{-2}$ would have produced a change of at least 3 mM at the enhancement wall-solution interface. Such an explanation is further supported by the fact that both coefficients were reduced to half in 10.0 mM KCl. (*b*) The actual value of $\beta$ chosen could be rather low, though even as much as a twofold increase in $\beta$ will only cause a decrease of 20% in the transport number component. (*c*) The value of $\sigma Lp$ chosen ($3.6 \times 10^{-5}$ cm· $sec^{-1}$ $atm^{-1}$) may be rather high and is in fact slightly higher than the values measured by Tazawa and Kamiya (1965) on *Nitella flexilis*.

*Concentration changes.* The concentration measured by electrode 2, at what was considered to be an effective distance of 1.64 mm from the cell wall, reached a maximum of about 1.3 mM KCl, with 1.0 mM KCl in the bulk of the medium, after a positive current pulse of 500 $\mu a \cdot cm^{-2}$ of 200 sec duration (Fig. 7). The time taken for the concentration at electrode 2 to reach a maximum (400 sec) after the current pulse corresponded quite well with that predicted for a distance of 1.64 mm (500 sec, cf. Fig. 7 of part I). The values calculated graphically for the relaxation of a concentration profile in a *semi-infinite medium* would imply a change in concentration of *at least* 2.7 mM at the enhancement wall-solution interface (Fig. 8 of part I). Correspondingly for a negative pulse, the concentration decreased to about 0.04 mM. Thus, the complete contribution due to the transport number effect at both sides of the membrane was about 10 $\mu l \cdot coul^{-1}$. The total coefficient of 20 $\mu l \cdot coul^{-1}$ calculated from these measured concentration changes is close to the directly observed

value of 23 $\mu$l. coul$^{-1}$. The maximum change in concentration measured at electrode 2 after various current pulses has been plotted in Fig. 7 as a function of pulse duration. As the pulse duration was increased to 100–200 sec, this change in concentration reached a maximum. This implied that after current had been passing through the wall for times greater than this, the concentration profiles set up across it had reached a steady state. These times are not very different from the observed times of 70–90 sec needed for the current-induced volume flows themselves to reach a maximum.

The concentration change across the cell wall may also be estimated from a measurement of the function $\Psi$. $\Psi$ will, however, underestimate this concentration difference. Primarily this will be because of the slight delay in recording the membrane PD which initially decreases very rapidly. Furthermore, as $\Delta C$ approaches $C$, if $\Delta C$ (enhancement) is greater than $\Delta C$ (depletion) $\Psi$ will underestimate the changes in concentration at the enhancement interface. Finally, since $\Psi$ is calculated assuming $t_K/t_{Cl} \gg 1$, a possible reduction of $t_K/t_{Cl}$ in the wall, as the concentration of the enhanced solution increases, may now cause an underestimate of $\Psi$ itself. Nevertheless, the calculated values of 0.7 and 1.4 $\pm$ 0.2 mM for current pulses of 100 and 500 $\mu$a $\cdot$ cm$^{-2}$ were not very different from the concentrations 1.0 and 3.0 mM needed to produce the required transport number component of flow. Also, $\Psi$ reached a maximum in about 50–80 sec (Fig. 10) which corresponds even more closely with times of 70–90 sec for the volume flow to reach a maximum.

Finally, the experiment showing the effect of solution replacement at one interface was again consistent with the two component nature of the current-induced flows; with one component being due to local osmotic flows.

*II. Whole Cells. Volume flows.* If the cell wall is neglected, $\alpha$ is taken as 0.5, $\beta$ = 4.0, and $\beta'$ = 20 cm$^{-1}$ (as discussed in the section on a comparison of experimental results with theoretical predictions and part I) then after about 200 sec the flow coefficient is about 25 $\mu$l $\cdot$ coul$^{-1}$ with a maximum theoretical value of about 36 $\mu$l $\cdot$ coul$^{-1}$. This should be compared with the experimental values of 10.8 $\pm$ 3.8 and 23.0 $\pm$ 6.4 $\mu$l $\cdot$ coul$^{-1}$ for hyperpolarizing and depolarizing current pulses respectively.

If the cell wall is considered the flow would be expected to reach a maximum much sooner. Assuming the diffusion coefficient for $K^+$ to be 5 $\times$ 10$^{-7}$ cm$^2$ sec$^{-1}$ (as estimated by Gaffey and Mullins, 1958), then, the contribution of the wall to the total coefficient would be about 15 $\mu$l $\cdot$ coul$^{-1}$ after 10 sec.

Thus, qualitatively it may be expected that concentration enhancement in the wall causes the flow to increase quite rapidly until the flow rate becomes equal to the internal interface maximum rate given by $\alpha I/FC_i$ (see the section on the transport number effect at a cylindrical membrane of part I). Qualitatively, this means that the loss or gain of solute at the internal interface due to the sweeping away effect, caused by the over-all flow, would then be equal to the gain or loss of solute due to the transport number effect at that interface. An increase in the flow component due to the

transport number effects in the wall would then be accompanied by a decrease in the component of flow due to the transport number effects at the internal interface as a result of increased sweeping away there. This will then tend to keep the flow at the constant rate determined by the feedback at the interior interface and equal to $\alpha I/FC_i$.

The predicted value of about 36 $\mu$l· coul$^{-1}$ for the maximum-rate coefficient is higher than observed. However, if $\alpha$ was less than 0.5, the discrepancy might be explained. Since it was noted that the coefficients varied considerably for hyperpolarizing and depolarizing pulses and seemed to decrease somewhat with increasing current, $\alpha$ might well have been lower, particularly if the tonoplast was the controlling membrane.

*Concentration changes.* The transient drifts in membrane PD which occur during the passage of constant current through *Chara* cells also support the model. Using the value of 1.0 m equivalent liter$^{-1}$ for the concentration of $K^+$ in the wall, for a cell in an external solution of 0.1 mM KCl, the drifts in potential predicted from the model in part I are shown in Fig. 17, and are compared with those measured ex-

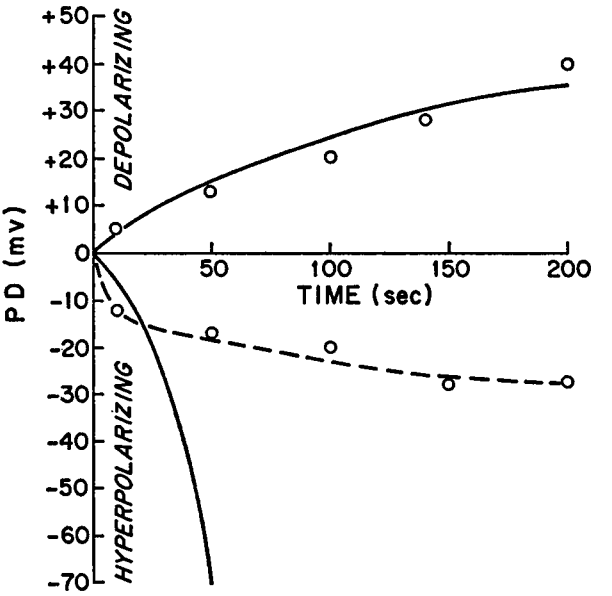


FIGURE 17 A comparison between the PD transients during a current pulse predicted theoretically for the wall-membrane model discussed in part I and those measured for a cell (4*I*) of *Chara australis* in 0.1 mM KCl. The theoretical curves (full lines) were calculated for the experimental current densities of 1.6 $\mu$a·cm$^{-2}$ (depolarizing) and 1.8 $\mu$a·cm$^{-2}$ (hyperpolarizing). The experimental points, *O*, also indicated in the hyperpolarizing case by a broken line, were obtained from the change in membrane potential immediately after current pulses of different duration (see Fig. 15).

perimentally. There is good agreement for depolarizing pulses, and for the first 20 sec for hyperpolarizing pulses (then $\Delta C \simeq 0.4\ C$). After this, the divergence is due to the fact that $\Delta C$ approaches $C$ and so, as discussed in part I, the analysis begins to break down, perhaps with $P_K$ decreasing as the PD becomes more negative. The concentrations calculated from such drifts indicate that the flows should reach a maximum in about 10–30 sec, somewhat lower than the 40–60 sec observed. This discrepancy could be due to the sweeping away effect inside the cell opposing the flow and therefore increasing the time taken for it to reach a maximum.

It has already been noted that for large hyperpolarizing pulses there were variations in the pattern of potential transients. The PD first increased slowly up to about $-340$ mv after which the PD suddenly started to decrease and in some cases became very unstable (Fig. 14 *b*) showing slow oscillations (2–3 sec period). The following explanation is suggested: due to the transport number effect in the wall, the concentration of $K^+$ decreases and the PD increases till it reaches the threshold for the nondestructive punch through breakdown observed by Coster (1965). He found that punch through invariably occurred between $-300$ and $-390$ mv for *Chara* and *Nitella* cells (Coster 1965, 1966 *b*). When this breakdown occurred, Coster showed that the membrane resistance decreased and the chloride permeability, $P_{Cl}$, increased. Such an increase in $P_{Cl}$ will cause a decrease in the transport number of $K^+$ in the membrane which if radical enough will allow the local $K^+$ profile to increase. As the $K^+$ concentration increases, so the membrane potential decreases (i.e. becomes less negative). Then, assuming a small hysteresis in the punch through threshold, the punch-through effect will again turn off, $P_{Cl}$ will drop, and the whole process will start again until punch through reoccurs. The slow oscillations were also noted by Coster (1966 *b*), who also favoured an explanation through a concentration-diffusion effect because of the time course involved.

## CONCLUSIONS

These experiments have shown conclusively that there is current-induced depletion and enhancement near membrane surfaces due to transport number discontinuities at the various interfaces. The resulting current-induced volume flows are therefore in general composed of two components: an electroosmotic one and one due to the transport number effect.

There was good agreement between the predictions from the theoretical models and the experimental observations, considering that the models were considerably simplified and that the magnitudes of certain parameters inferred from data published for other *Characean* cells could be slightly different from those for *Chara australis*.

The transport number effect, therefore, should always be considered whenever there are discontinuities in transport numbers at any membrane-solution interface. It will result in both a current-induced volume flow and transient changes in mem-

brane PD, both during, and persisting for a short while after the passage of current. It may often be a possible mechanism for various transient changes in potential (as in the example of punch through oscillations already noted) and in any case should always be allowed for. In particular, these experiments have also shown that for cell walls the true electroosmotic component contributed about 10 $\mu l \cdot coul^{-1}$ (53 moles·Faraday$^{-1}$) to a total (electroosmotic and transport number effect) of 23 $\mu l \cdot coul^{-1}$ (112 moles·Faraday$^{-1}$). For whole cells the average electroosmotic component for both hyperpolarizing and depolarizing pulses contributed about 7.2 $\mu l \cdot coul^{-1}$ (38 moles·Faraday$^{-1}$) to a total of about 17 $\mu l \cdot coul^{-1}$ (100 moles. Faraday$^{-1}$).

These electroosmotic coupling coefficients quoted for whole cells were measured effectively across cell walls and cell membranes in series, and Briggs (1967) has recently asked the important question as to whether or not the electroosmotic coupling in the wall is enough to account for the whole electroosmotic flow across the composite system of walls and membranes. We have made some calculations of the effect of the wall from the parameters that we have measured and estimate that the direct contribution of the cell membranes to electroosmosis is about 80% of the total measured coefficient of the composite system. This will be published later in more detail.

It is of interest that recently Vargas (1967), in an analysis of streaming potentials in the squid giant axon has shown that they too are composed of two components, as instantaneous component and then a diffusion potential component similar to the sweeping-away effect which is discussed here. He found that the true streaming potential also comprised only about 30% of the total change in potential.

Fensom, Ursino, and Nelson (1967) have measured current-induced flows of water in *Nitella* and claim to have detected changes in membrane pore size due to various treatments. Unless it can be shown that the current-induced flows in these experiments were wholly due to electroosmosis, the conclusions made by these authors may be entirely wrong. If, for example, indoleacetic acid caused changes in the transport numbers of cations in the membrane or cell wall or changes in hydraulic conductivity of the membrane, changes in local osmosis might account for the apparent change in "electroosmotic efficiency". Furthermore, the differences in current-induced water flow when various cations are placed in the medium in turn may well be due to the same cause, namely differences in the transport number effect.

We would like to thank Dr. E. M. Wright and Dr. J. M. Diamond for a critical reading of the manuscript. We are also grateful to Mr. A. Young for the basic design of the main phototransducer amplifier and to George Brown and Co. Pty, Ltd. (Sydney) for the design of the stabilized supply for the backing-off circuit.

P. H. Barry was the holder of research studentships from the (Australian) Commonwealth Scientific and Industrial Research Organisation (CSIRO) and Flinders University during the course of this work. The work was carried out at both the University of Sydney and Flinders University and is included in part II of a Ph.D. Thesis (Barry, 1967). We are also grateful for an extra-mural grant from the C.S.I.R.O. to the Biophysics Laboratory, Flinders University and for the support of the Australian Research Grants Committee.

Dr. Barry's present address is the Physiology Department, School of Medicine, Center for Health Sciences, University of California, Los Angeles, California 90024.

## APPENDIX

### *Time Course for Pure Electroosmatic Coupling*

As far as electroosmosis is concerned, provided there is a restraint on the concentration of ions in the membrane, such as anion exclusion, then both the pore and frictional models imply almost an instantaneous (i.e. $< 10^{-6}$ sec) achievement of maximum flow following the onset of a current pulse.

For the pore model the time constant would be $< 10^{-12}$ sec, the time needed for Poiseuille flow to become established in a pore less than 100 A. This may be shown to be given by $\tau \simeq \rho a^2/\eta\alpha_1^2$ where $\rho$ = density of the pore fluid, $a$ is the pore radius, $\eta$ is the viscosity of pore fluid considered similar to water, and $\alpha_1$ is the first zero of the Bessel function $J_0(\alpha)$. Even the possibility of a considerable increase in effective viscosity will still leave the time constant infinitesimally small.

Similarly, the basic nature of frictional models would imply that maximum flow should be accomplished in at most $10^{-7}$ seconds, which is the relaxation time of conduction ions in a 1.0 mM electrolyte (Glasstone, 1948).

### *Time Required for Current to Reach a Maximum*

An analysis of a charging circuit with a series resistance $R$, passing a current across a cell membrane (surface area $A$) of resistance $r$ ($\Omega$ cm$^2$) and capacity $C$ ($\mu$F·cm$^{-2}$), in parallel, indicates that the charging time constant, $\tau$, for current actually flowing across the membrane (not including the capacitative current, which will not contribute to electroosmotic coupling), will be given by

$$\tau = \frac{RrC}{r/A + R}$$

For the cells of *Chara australis* used where

$$r \cong 10 \text{ k}\Omega \cdot \text{cm}^2$$

$$C \cong 1 \ \mu F \cdot \text{cm}^{-2}$$

$$A \gtrsim 1 \text{ cm}^2$$

$$R \gtrsim 1 \ M\Omega.$$

then

$$\tau \cong 10 \text{ m sec.}$$

*Received for publication 9 August 1968 and in revised form 25 November 1968.*

## BIBLIOGRAPHY


BARRY, P. H. 1967. Investigation of the movement of water and ions in plant cell membranes. Ph.D Thesis. University of Sydney, Sydney, Australia.

BARRY, P. H. AND A. B. HOPE. 1969. *Biophys. J.* **9**:700.

BRIGGS, G. E., A. B. HOPE, and R. N. ROBERTSON. 1961. Electrolytes and Plant Cells. Blackwell Scientific Publications, Oxford, England.

COLE, G. H. A. 1962. Fluid Dynamics. Methuen Monographs on Physical Subjects. Methuen and Co., Ltd., London, England.

COSTER, H. G. L. 1965. *Biophys. J.* **5**(5):669.

COSTER, H. G. L. 1966 *a*. *Aust. J. Biol. Sci.* **19**:545.

COSTER, H. G. L. 1966 *b*. Ionic relations and the electrical properties of the membranes of giant algal cells. Ph.D. Thesis. University of Sydney, Sydney, Australia.

DAINTY, J., and A. B. HOPE. 1959. *Aust. J. Biol. Sci.* **12**(2):136.

DAINTY, J., A. B. HOPE, and C. DENBY. 1960. *Aust. J. Biol. Sci.* **13**(3):267.

FENSOM, D. S., and J. DAINTY. 1963. *Can. J. Bot.* **41**:685.

FENSOM, D. S., D. J. URSINO, and C. D. NELSON. 1967. *Can. J. Bot.* **45**:1267.

FINDLAY, G. P. and A. B. HOPE. 1964 *a*. *Aust. J. Biol. Sci.* **17**(1):62.

FINDLAY, G. P. and A. B. HOPE. 1964 *b*. *Aust. J. Biol. Sci.* **17**(2):400.

GAFFEY, C. T., and L. J. MULLINS. 1958. *J. Physiol.* **144**:505.

GLASSTONE, S. 1948. Textbook of Physical Chemistry. Macmillan and Co., London, England. 2nd edition.

KAMIYA, N., and M. TAZAWA. 1956. *Protoplasma.* **46**(1–4):394.

KISHIMOTO, U., and M. TAZAWA. 1965. *Plant Cell Physiol.* **6**:507.

MACKAY, D., and P. MEARES. 1959. *Trans. Faraday Soc.* **55**(2):1221.

MAILMAN, D. S., and L. J. MULLINS. 1966. *Aust. J. Biol. Sci.* **19**:385.

OSTERHOUT, W. J. V. 1949. *J. Gen. Physiol.* **32**:553.

TAZAWA, M., and Y. NISHIZAKI. 1956. *Jap. J. Bot.* **15**(2):227.

TAZAWA, M., and N. KAMIYA. 1965. *Ann. Report of Biol. Works.* Faculty of Science, Osaka University. **13**:123.

VARGAS, F. 1968. *J. Gen. Physiol.* **51**(5):123.